

12TH NORTH AMERICAN MASONRY CONFERENCE

Masonry: Science • Craft • Art

Denver, Colorado May 17 - 20, 2015

Blast loading of masonry infills: testing and simulation

João M. Pereira¹, José A. Campos² and Paulo B. Lourenço³

Abstract

This work intends to present a newly developed test setup for dynamic out-of-plane loading using underWater Blast Wave Generators (WBWG) as loading source. Underwater blasting operations have been, during the last decades, subject of research and development of maritime blasting operations (including torpedo studies), aquarium tests for the measurement of blasting energy of industrial explosives and confined underwater blast wave generators. WBWG allow a wide range for the produced blast impulse and surface area distribution. It also avoids the generation of high velocity fragments and reduces atmospheric sound wave. A first objective of this work is to study the behavior of masonry infill walls subjected to blast loading. Three different masonry walls are to be studied, namely unreinforced masonry infill walls and two different reinforcement solutions. These solutions have been studied previously for seismic action mitigation. Subsequently, the walls will be simulated using an explicit finite element code for validation and parametric studies. Finally, a tool to help designers to make informed decisions on the use of infills under blast loading will be presented.

Keywords: Infill walls, Out-of-plane loading, Blast Loading, WBWG

¹ PhD, ISISE – Institute for Sustainability and Innovation in Structural Engineering, University of Minho, Portugal, jpereira@civil.uminho.pt

² Professor, Department of Mechanical Engineering, University of Coimbra, Portugal, Andrade.campos@dem.uc.pt

³ Full Professor, ISISE – Institute for Sustainability and Innovation in Structural Engineering, University of Minho, Portugal, pbl@civil.uminho.pt

Introduction

Very few numerical or experimental studies have been conducted on impact and blast on structural components of building structures, characterized by strain rates well over 1 s^{-1} , with quasi-static tests characterized by strain rates in the range 10^{-5} to 10^{-7} s^{-1} . This calls for more research to obtain an accurate representation of the effect of blasts, as high nonlinear behavior and possible brittle failure has been observed. The vulnerability of structures under dynamic actions has been emphasized by many studies, most of them performed to mitigate seismic risk. The out of plane vulnerability of the masonry envelop under dynamic loading is considered critical due to the risk of loss of lives, emphasized by many studies, particularly in the case of earthquakes [Calvi and Bolognini 2001] and explosion debris [Wu and Hao 2007]. Still, only a few laboratory experimental investigations are available, simulating vehicles impacts on parapets [Gilbert et al 2002] and air-blasting [Mayrhofer 2002].

The main issue on the mechanical behavior under blast is the strength increase due to high-strain rate. Explosions produce very high strain rates, usually around 10^2 – 10^4 s^{-1} . Reinforced concrete structures, for example, are highly affected by this phenomenon. Its resistance can increase greatly due to the high strain rate effect, dynamic increase factor as high as 4 in compression and 6 in tension have been reported [Grote et al 2001, Ngo et al 2004]. In the case of masonry and its components the available studies are very limited. Recently, dynamic increase factors higher than 2 in compression for clay brick were reported [Hao and Tarasov 2008, Pereira et al 2013].

This work intends to present a newly developed test setup for testing out-of-plane walls under dynamic loading using underwater blast wave generators. Underwater blasting operations have been, during the last decades, subject of research and development of maritime blasting operations (including torpedo studies), of aquarium tests for the measurement of blasting energy of industrial explosives and of confined underwater blast wave generators (WBWG). WBWGs allow a wide range of produced blast impulses and surface area distributions. This technique avoids also the generation of high velocity fragments and reduces atmospheric sound wave [Tavares et al 2012, Ambrósio et al 2013].

Test Setup

This work was performed in collaboration with LEDap (Laboratory of Energetics and Detonics) in Condeixa-a-Nova, Portugal. The developed test setup was constructed at LEDap facilities and comprises several elements. A support steel structure holds the structural element in place and provides sufficient reaction to the wall's reinforced concrete frame (Figure 1a). On one side of the wall a number of large (one cubic meter) water containers are placed to act as WBWG and apply the desired load. On the other side of the wall, measuring equipment is placed in order to obtain the required behavior of the wall. The maximum deflection is measured using laser and high speed video equipment, which was used to study the behavior of the wall during the test, Figure 1a. This area is surrounded by protection walls and a safe area was placed to provide secured hosting for the acquisition equipment and personal during the tests, Figure 1b.

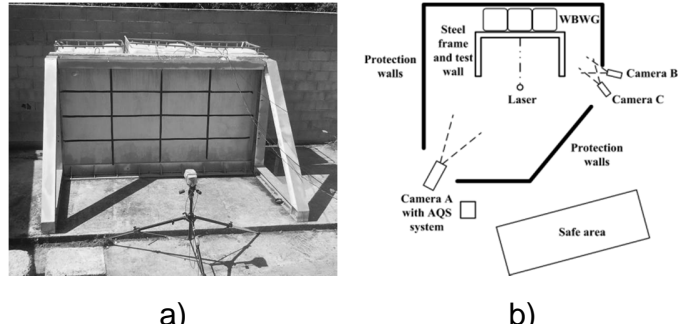


Figure 1. Final configuration of the test site: a) supporting structure and wall; b) test setup layout.

Blast Wave Generators

The original blast wave generators (BWG), from the direct application of an explosion in air or high explosives, have the inconvenient of hot polluted gases products, a reduced area of induced pressure, the possibility of generation of high velocity fragments and the existing of a very intense sound wave [Tavares et al 2012]. Since physical properties of water and air are different, the characteristics of the shock waves (in air and water) are different, mainly due to the differences of density and shock wave velocity (shock impedance). After the detonation of an explosive charge under water, the detonation products expand generating a shock wave in water and forming a gas bubble. Gas bubble expands and pressure inside the bubble decreases. Because of inertia of water flow in front of the bubble, the expansion of gas bubble continues even after the slightly decrease of pressure inside the bubble to a value below pressure of the surrounding water. Afterwards, the pressure inside the gas bubble drops below pressure of surrounding water and gas bubble movement stops. However the phenomenon does not stops - gas bubble contracts under the action of surrounding pressure [Ambrósio et al 2013]. This kind of evolutions is very important in large volumes, but in our case it must be reduced or even eliminated – in this case the water should be used just as a pressure dissipative medium, see Figure 2.

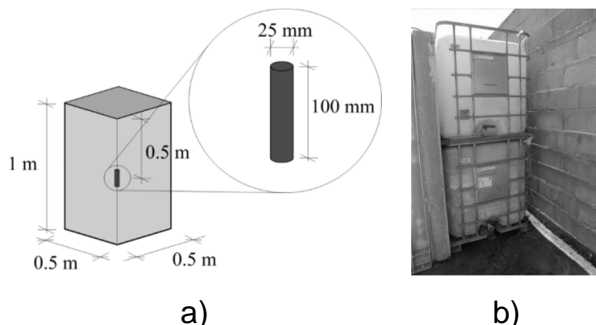


Figure 2. WBWG: a) explosive charge location; b) placing the water container in its final position.

Pressure/deflection Acquisition

One of the main issues regarding dynamic testing, blast loading in this case, is the proper acquisition of signals. The measuring equipment needs to have capacity for high acquisition rates. In this work there were two signals that need to be recorded: a) the pressure profile acting on the wall; and b) the deflection profile of the wall.

For the pressure acquisition, a new sensor was developed for these tests. The mechanism used to measure the pressure consists in an assembled instrumental stainless steel plate between the wall and the water container. The pressure setup is a pressure tube connected to a pressure sensor. This tube contains thin oil and is connected in a closed loop, Figure 3. The pressure device works like a force multiplier justified by the hydrostatic pressure transmission. The pressure sensors used were 4-20 mA GemsTM Sensors and Controls 3100B0016G01B and 3100B0010B01B. In order to plot the acquired pressure signal, these sensors were connected to Tektronix TDS 320 oscilloscopes. This sensor was previously tested and calibrated [Tavares et al 2012, Ambrósio et al 2013].

For the deflection acquisition, a Keyence CMOS Multi-Function analogue laser sensor IL-2000 with a signal amplifier IL-1000 was used (Figure 4a). This sensor was connected to a National Instruments acquisition system composed of a SCXI-1000DC chassis, a SCXI-1600 data acquisition and control card for PC connection and a generic input module SCXI-1520 with a SCXI-1314 mount. In this case the sampling speed was limited by the laser sensor and was set as 3 kHz. With this system, it is only possible to measure the deflection of one point in the wall.

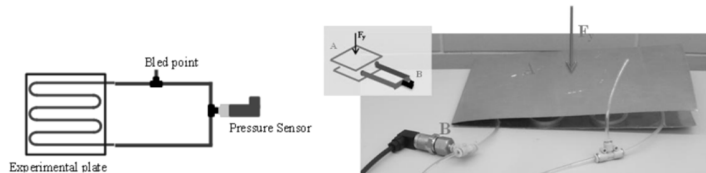


Figure 3. Pressure sensor schematics and construction.

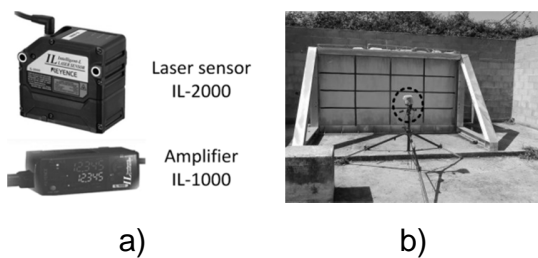


Figure 4. Deflection acquisition: a) laser sensor and amplifier; b) laser mounted in place.

Besides the usage of pressure and displacement transducers, high speed video equipment was used to study the behaviour of the wall during the test. Three different cameras were used, marked in Figure 1b as camera A, B and C. Camera A is a PHOTRON APX-RS and was placed to have a full view of the wall. This camera was set with an acquisition frequency of 1 kHz. Cameras B and C are Casio EX-FH25 and were placed with different views. Camera B was placed on the side of the wall in order to capture the profile of the wall.

Camera C was placed in order to capture the WBWG and their behaviour during the test. Both these two cameras were set with an acquisition frequency of 0.4 kHz. To help having a better view of the movement of the wall, a regular mesh was drawn in the wall using black tape, Figure 4b.

Unreinforced Infill Wall

The first specimen tested with this new developed test setup was an unreinforced masonry wall. This wall was a $3.5 \times 1.7 \text{ m}^2$ masonry panel inside a reinforced concrete frame with a thickness of 180 mm, 150 mm from the hollow clay block and 15 mm on each side from plaster. This wall specimen was tested previously in different condition and additional details on the composition and the construction procedure of this specimen can be found in [Pereira et al 2011, Pereira 2013].

After the test, the acquired signals need to be processed. From the oscilloscopes the applied pressure on the wall was obtained and the final pressure profile was plotted, Figure 5a. The pressure rises to 149 kPa in the first 6 ms, then decays and reaches 119 kPa at 17.5 ms and stops acting after 29 ms. From the laser sensor, the deflection on the central point of the wall was obtained, Figure 5b. The deflection on the wall has an expected profile, increasing until its maximum of 14.6 mm after 24 ms and has a residual deformation of around 10 mm. These results were used to calibrate numerical models able to simulate these extreme dynamic situations, which allow having a more detailed study on these structural elements.

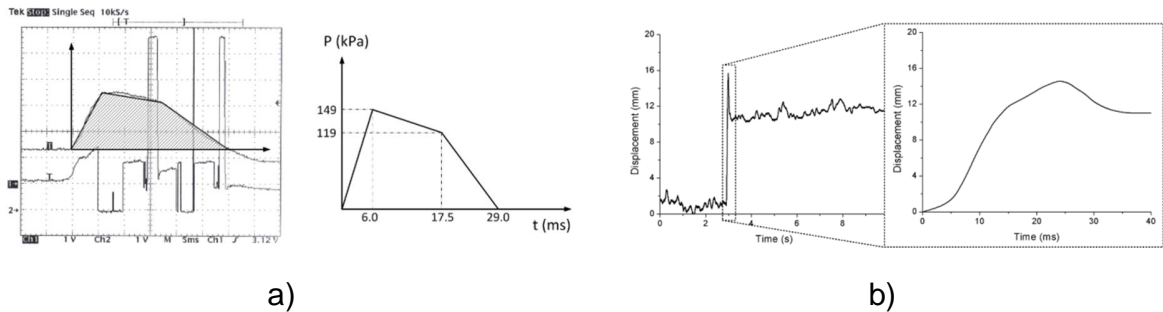


Figure 5. Acquired signals: a) pressure profile; b) displacement profile.

Numerical Modeling

The FEM model was built in the ABAQUS software [Abaqus 2010], where the explicit solver was used. This software has been used successfully in previous situation regarding similar loading conditions [Cabello 2011, Heidarpour et al 2012] and similar materials [Zhen et al 2010, Al-Gohi et al 2012]. This wall was discretized with 8 nodes solid elements (C3D8R) with reduced integration and hourglass control [Abaqus 2010]. The final mesh was automatically generated by ABAQUS, and then manipulated and controlled in order to obtain a good quality mesh. Only the infill masonry was modelled and all edges were considered constrained in all degrees of freedom. The thickness of the wall was set as 180 mm (brick plus plaster). The final mesh has 4872 elements and 6844 nodes

The CDP (Concrete Damaged Plasticity) material model used in ABAQUS software is a modification of the Drucker-Prager strength hypothesis. The CDP model assumes that the failure in both tensile cracking and compressive crushing of the material is characterized by damage plasticity. Additional details on this material model can be found in [Abaqus 2010, Lubliner et al 1989]. Table 1 presents the static mechanical properties for this masonry infill wall and were obtained from [Pereira 2013]. These values served as a base for the calibration of the numerical model. The dynamic properties were obtained by calibrating the numerical model to match the deflection behaviour of the experimental wall. The final dynamic properties and the respective dynamic increase factor (DIF), which is the relation between the dynamic properties and its static reference, can be seen in Table 1.

Figure 6a shows the result of the numerical model and compares it with the experimental results. There is a good initial agreement up until 12 mm in deformation. At this instant the experimental curve changes its slope, probably due to appearing cracks. The maximum displacement has a difference of 3%. In the post-peak behaviour there is a considerable difference between the experimental and the numerical model. In the experimental test the wall was able to set its residual deformation at 76% of the maximum deformation. In the numerical model the residual deformation was 91%. In the experimental test, when the blast wave from the WBWG reaches the wall it generates an expansion wave that travels through the thickness of the wall. When this expansion wave reaches the opposite edge of the wall it will start moving in the opposite direction creating a “negative” wave profile, which was not considered in the numerical model. When the structural element reaches a high level of deformation this effect can be neglected, due to the lack of capacity of the element to sustain this expansion wave in the opposite direction.

Table 1. Mechanical properties for masonry wall.

Masonry	Static Ref.	Calibrated	DIF
Compressive Strength (fc) [MPa]	1.26	3.78	3
Tensile Strength (ft) [MPa]	0.125	0.375	3
Mode I-fracture energy (G _{fI}) [N/mm]	0.012	0.025	2
Young's Modulus (E) [GPa]	3.6	7.2	2

A proper definition of the mechanical properties through the dynamic increase factor is crucial in this type of analysis. As can be seen in Figure 6b, where a comparison of the dynamic increase factor is performed, using the static properties (DIF=1) in this model results in excessive deformation which would result in the collapse of the wall. On the other hand, using a dynamic increase factor of 5 in all mechanical properties the wall behaves mostly in its elastic regime, having a neglectable residual deformation.

Besides the comparison of the deflection profile, the damage on the wall was also compared. In order to have an approximation on where the cracks would appear, the maximum principal plastic strains were plotted, Figure 7a. As expected, according to this model, there is a concentration of cracks at mid height of the wall that will start to spread to the corners as we move further from the center point. There is also some damage at the bottom and top edge of

the wall. These results are in agreement with the observed damage in the experimental test, Figure 7b.

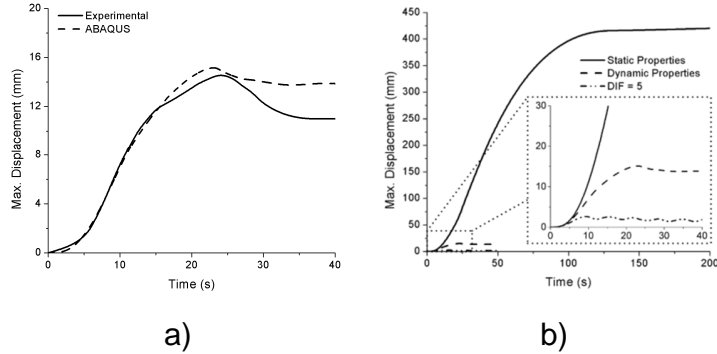


Figure 6. Numerical results: a) comparison between the numerical and experimental results; b) influence of the dynamic increase factors on the behavior of the wall.

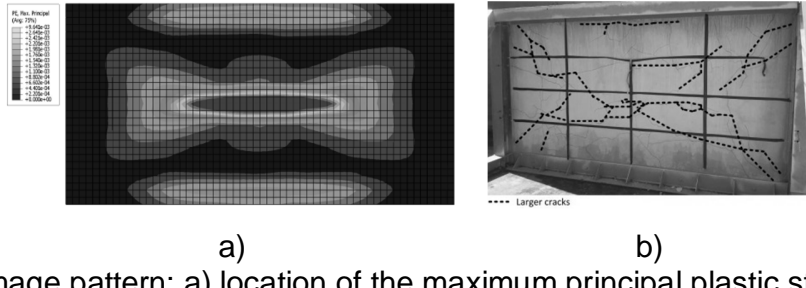


Figure 7. Damage pattern: a) location of the maximum principal plastic strains; b) larger cracks after the test.

Parametric Study

A parametric study was performed on the mechanical and geometric properties of unreinforced masonry infill panels. The results are summarized in Figure 8. The maximum displacement is plotted against the scaled distance, Z :

$$Z = \frac{R}{W^{1/3}} \quad [1]$$

Where R = distance to the explosive and W = mass of the explosive in TNT equivalent.

To create the pressure profiles when varying the weight of the explosive or the distance, a set of empirical solution are available in the literature [Bangash and Bangash 2006]. The pressure profile was assumed to be with a triangular shape with the maximum pressure at the initial time and decaying in pressure until the positive duration.

The compressive strength, Figure 8a, has a considerable influence on the maximum displacement of the wall, for smaller scaled distances. This influence appears to fade once a certain level of compressive strength is achieved. Meaning that from a certain point there is no real advantage on increasing the compressive strength. The same conclusion can be obtained when analysing the tensile strength, Figure 8b. When varying the tensile strength, the fracture energy was also changed in the same proportion as the tensile strength. The Young's modulus, Figure 8c, influences the maximum displacement of the wall at all levels of

scaled distance. The Mode I-fracture energy, Figure 8d, only influences the maximum displacement at smaller scaled distances. Here, the tensile strength was kept the same for all models. The thickness of the wall, Figure 8e, is obviously one of the parameters with larger influence on the maximum displacement of the wall.

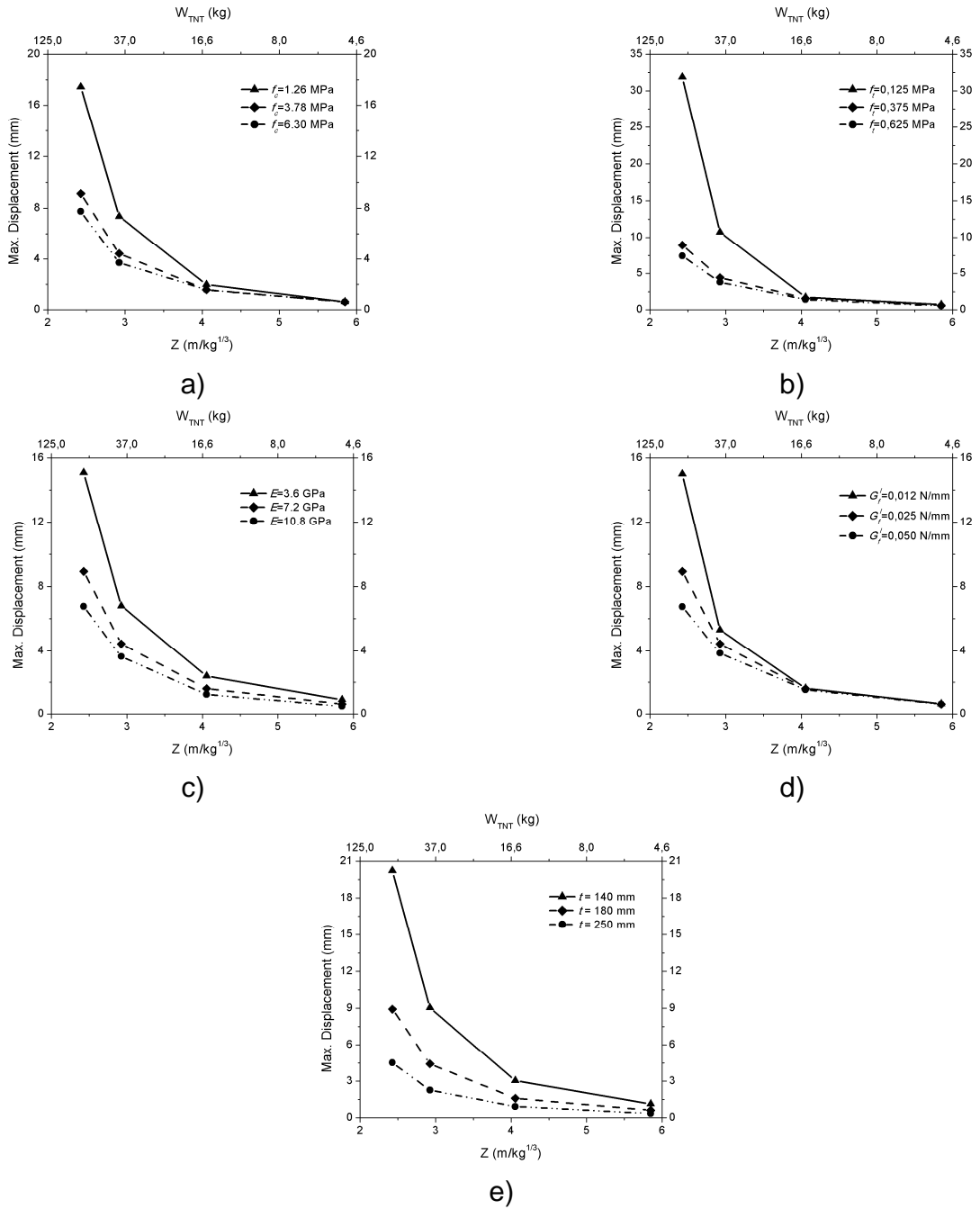


Figure 8. Parametric study on the properties of infill walls subjected to blast loading:
a) Compressive strength; b) Tensile strength; c) Young's modulus; d) Mode I-fracture energy;
e) Thickness of the wall.

Pressure-Impulse Diagrams

Pressure-Impulse diagrams are empirical tools that allow a given load-impulse combination, which will cause a specific level of damage, to be assessed readily [Cormie et al 2009]. These diagrams can be used to assess a specific loading profile which caused certain damage to an element, in a post-disaster scenario. On the other hand, these tools can be used at an early design stage to get an approximation of the damage to an element given a specific loading profile.

In order to make it easier for the designer to use these tools, for the structural elements under study, it is better to have damage criteria (Table 2) instead of pure deflection curves. For the present work, the criteria defined by [UFC 3-340-02 2008] will be applied, meaning that instead of iso-deflection curves, the P-I diagrams were plotted with two levels of damage, reusable and non-reusable. With the FE model calibrated, several simulations were performed for different levels of overpressures and impulses. For these numerical models a 1:1 scale was used, meaning that the masonry infill panels have an area of 5250 by 2550 mm². Two different masonry infill panels were studied, with 180 mm thickness and 230 mm thickness.

Although it was not possible to test experimentally reinforced solutions for the infill masonry walls, as done by [Pereira 2013], numerical models for the planned reinforced solutions were prepared. The first reinforcement solution under study – JAR: bed joint reinforcement – has BEKAERT MURFOR RND .4/100 every two horizontal joints. The second solution for reinforcement under study – RAR: external mesh reinforcement – has BEKAERT – ARMANET Ø1.05 mm 12.7×12.7 mm in both sides of the wall, embedded in the plaster. The reinforcement elements, for both models, were truss elements T3D2 [Abaqus 2010] and the material was considered to be elastic – ideal plastic with a tensile strength of 400 MPa and a Young's modulus of 210 GPa.

Table 2. Masonry damage criteria [UFC 3-340-02 2008].

Element	Yield pattern	Maximum support rotation
Masonry Reusable	One-way	0.5°
	Two-way	0.5°
Masonry Non-reusable	One-way	1.0°
	Two-way	2.0°

Figure 9 to Figure 11 present the obtained pressure-impulse diagrams for the three constructive solutions under study. As expected, the reinforced solutions are able to accommodate somewhat larger loading profiles and have the non-reusable and the reusable curves further away. Of course, higher percentages of reinforcement can be used to obtain a specified performance but, here, the focus is given to the minimum amounts of reinforcement. If the damage level required is the reusable stage, there is no real advantage in using the minimum reinforcement solutions, for weak masonry infills and large panels. Only at the non-reusable stage the minimum reinforcement solutions have a relevant contribution for the wall's response. These P-I diagrams can be used to select the proper constructive solution regarding a specific level of blast loading under design. As can be seen from Figure 8 to

Figure 11, the thickness of the wall is one important aspect to account for. The grid reinforcement is the solution with the highest mechanical improvement regarding the maximum displacement of the wall. Another important aspect regarding this reinforcement solution is that it also protects against the appearance of flying debris into, possibly, occupied areas.

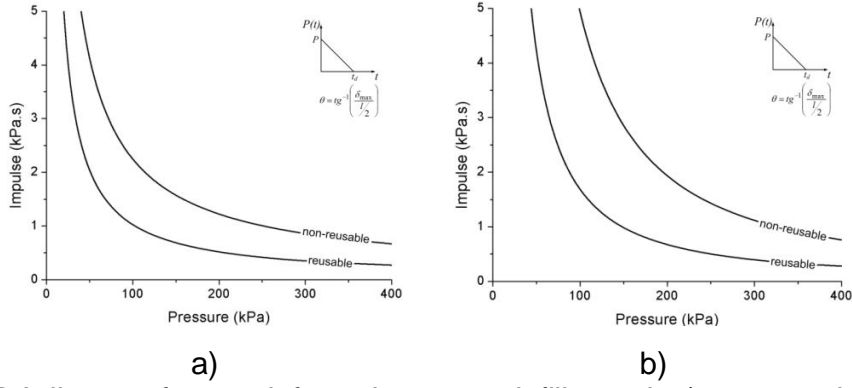


Figure 9. P-I diagram for unreinforced masonry infill panel: a) 180 mm; b) 230 mm.

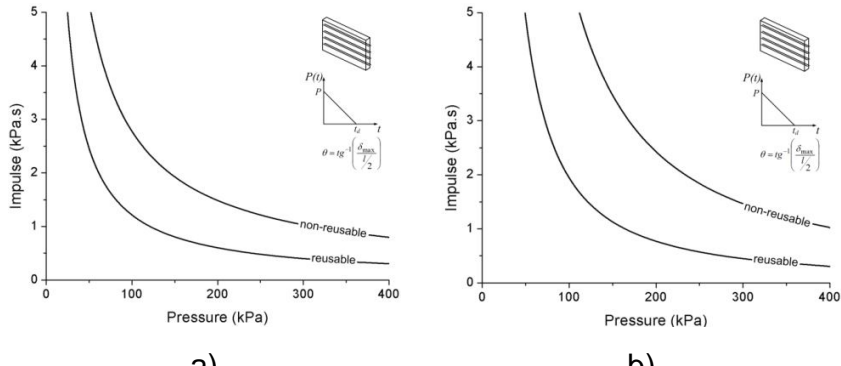


Figure 10. P-I diagram for masonry infill panel with minimum bed joint reinforcement: a) 180 mm; b) 230 mm.

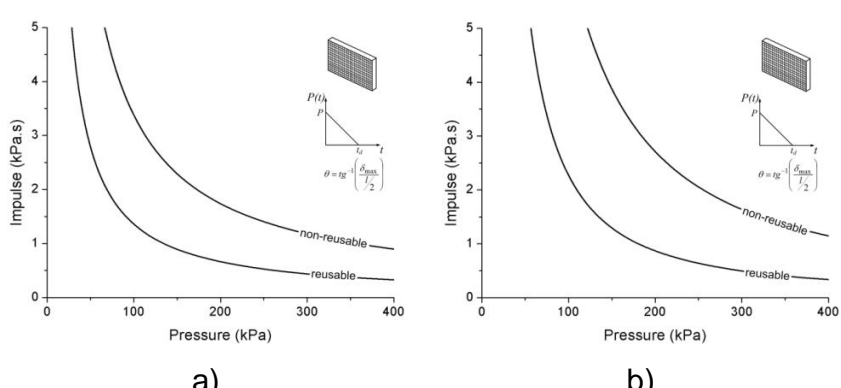


Figure 11. P-I diagram for masonry infill panel with minimum grid reinforcement in the plaster: a) 180 mm; b) 230 mm.

Conclusions

A newly developed test setup for dynamic out-of-plane testing on walls was presented, including the developed sensors and acquisition apparatus. One unreinforced masonry infill panel was tested under blast loading using underwater blast wave generators and the results were presented. The obtained results were used to calibrate a numerical model using ABAQUS Explicit dynamics software. A good agreement between the numerical model and the experimental data was obtained, allowing a more comprised study on this kind of masonry panels under dynamic out-of-plane loading in the form of a parametric study for different loading conditions. There is a point where the increase of the compressive and tensile strength is no longer effective, and the Young's modulus and the wall thickness are the parameters with the higher influence on the behaviour of the wall panel.

These results were used to create empirical tools – Pressure-Impulse diagrams – which can help the designer to estimate the response of the element under different loading conditions. It was shown that the use of these (low percentage) reinforcement solutions is more effective considering the non-reusable stage of the element. If the requirement is the reusable stage there is no real advantage in the use of these (low percentage) reinforcement solutions, and the best way to improve the response of the wall would be increasing its thickness or designing the reinforcement according to the performance sought. More experimental data is required to confirm these findings and additional masonry infill walls should be tested.

Acknowledgements

This work was performed under Project CH-SECURE funded by the Portuguese Foundation of Science and Technology – FCT. The authors acknowledge the support. The first author also acknowledges the support from his PhD FCT grant.

References

- Abaqus 2010: Abaqus user manual, Dassault Systems Simulia Corporation, Providence USA, 2010.
- Al-Gohi et al 2012: Al-Gohi, B.H., Demir, C., Ilki, A., Baluch, M.H., Rahman, M.K., Al-Gadhib, A.H., Seismic vulnerability of multi-leaf heritage masonry walls using elasto-plastic damage model. In: Proc. of the International Workshop: Role of research infrastructure in seismic rehabilitation. Turkey, 2012.
- Ambrósio et al 2013: Ambrósio, J., Ferreira, R., Mendes, R., Campos, J., Pereira, J.M., Lourenço, P.B., Prediction and experimental results of confined underwater blasting generators. In: Proc. of the 44th International Conference of the Fraunhofer ICT, Germany 2013.
- Bangash and Bangash 2006: Bangash, M.Y.H., Bangash, T., Explosions – Resistant buildings: Design analysis and case studies. Springer publications, Germany 2006.
- Cabello 2011: Cabello, B., Dynamic stress analysis of the effect of air blast wave on stainless steel plates. Msc-Thesis, Faculty of Rensselaer Polytechnic Institute 2011.

- Calvi and Bolognini 2001: Calvi, G.M., Bolognini, D., Seismic response of reinforced concrete frames infilled with weakly reinforced masonry panels. Journal of Earthquake Engineering, 5 (2001) 2, 153-185.
- Gilbert et al 2002: Gilbert, M., Hobbs, B., Molyneaux, T.C.K.: The performance of unreinforced masonry walls subjected to low-velocity impacts: experiments. International Journal of Impact Engineering, 27 (2002), 231-251.
- Grote et al 2001: Grote, D., Park, S., Zhou, M.: Dynamic behaviour of concrete at high strain rates and pressures. International Journal of Impact Engineering, 25 (2001) 9, 869-886.
- Hao and Tarasov 2008: Hao, H., Tarasov, B.G., Experimental study of dynamic material properties of clay brick and mortar at different strain rates. Australian Journal of Structural Engineering, 8 (2008), 117-132.
- Heidarpour et al 2012: Heidarpour, A., Bradford, M.A., Liu, J., Steel arches subjected to blast loading: a non-discretization analysis approach. Applied Mathematical Modelling, 36 (2012) 9, 3971-3984.
- Lubliner et al 1989: Lubliner, J., Oliver, S., Onate, E., A plastic-damage model for concrete. International Journal of Solids and Structures, 25 (1989) 3, 299-326.
- Mayrhofer 2002: Mayrhofer, C.: Reinforced masonry walls under blast loading. International Journal of Mechanical Sciences, 44 (2002), 1067-1080.
- Ngo et al 2004: Ngo, T., Mendis, P., Hongwei, M., Mak, S.: High strain rate behaviour of concrete cylinders subjected to uniaxial compressive impact loading. In: Proc. of the 18th Australasian Conference on Mechanics of Structures and Materials. Australia 2004.
- Pereira et al 2012: Pereira, M.F.P., Pereira, M.F.N., Ferreira, J.E.D., Lourenço, P.B., Behaviour of damaged masonry infill panels in RC frames subjected to out of plane loads. In: Proc. of the 7th International Conference on Analytical Models and New Concepts in Concrete and Masonry Structures. Poland 2011.
- Pereira et al 2013: Pereira, J.M., Dias, A., Lourenço, P.B., Dynamic properties of clay brick at different strain rates. In: Proc. of the 12th Canadian Masonry Symposium. Canada 2013.
- Pereira 2013: Pereira, M.F.P.: Avaliação do desempenho das envolventes dos edifícios face à acção dos sismos (in Portuguese). PhD-Thesis, University of Minho, 2013. Department of Civil Engineering: Guimarães 2013.
- Tavares et al 2012: Tavares, B., Mendes, R., Plaksin, I., Campos, J., Santos, P.M.S., Duarte, B.P.M., Oliveira, N.M.C., Pereira, J.M., Lourenço, P.B., Prediction and experimental results of confined underwater blasting generators. In: Proc. of the 2nd Korean International Symposium on High Energy Materials – KISHEM. Korea 2012.
- UFC 3-340-02 2008: UFC 3-340-02: Structures to resist the effect of accidental explosions. Department of Defense, USA 2008.
- Wu and Hao 2007: Wu, C., Hao, H., Safe scaled distance for masonry infilled RC frame structures subjected to airblast loads. Journal of Performance of Constructed Facilities, 21 (2007) 6, 422-431.
- Zhen et al 2010: Zheng, Y., Taylor, S., Robinson, D., Nonlinear finite element analysis of masonry arch bridges reinforced with FRP. In: Proc. of the 6th International Conference on Arch Bridges – ARCH'10. China, 2010.